Aircraft Mission Analysis Enhancement by Using Data Science and Machine Learning Techniques

Junghyun Kim[1], Seulki Kim[2], Kisun Song[2], Yongchang Li[3], and Dimitri N. Mavris[4]

Georgia Institute of Technology, Atlanta, Georgia, 30318, United States

As air-traffic demand continues to grow, it is expected that there will be a growing need for optimizing fuel consumption to airlines. To that end, it is pre-requisite to estimate fuel consumption as accurate as possible. However, most of the aircraft operation datasets have been elusive due to proprietary purposes. Under these circumstances, a comprehensive software dubbed the Aviation Environmental Design Tool (AEDT) has been prevalently used by many aerospace engineers to calculate the fuel consumption. It is highly hypothesized that, besides, if the AEDT could collaborate with reliable weather information, its modeling fidelity would be enhanced. In this paper, we proposed a novel aircraft mission analysis framework by incorporating data-driven approaches with the AEDT and state-of-the-art machine learning (ML) techniques to improve the accuracy of aircraft mission analysis. As the source of weather information, the world-wide weather dataset called MERRA-2 was regressed by a Support Vector Machine (SVM) along the time and three-dimensional coordinates in the entire US territory. The created SVM model successfully provided continuous behavior of weather, showing a good agreement to the reference data. As the final research, a four-dimensional (4-D) flight trajectory of operations in several sampled airports has been retrieved from external public databases and integrated with corresponding weather information extracted from the SVM model. Finally, it was observed that the collaboration of the SVM weather model and the AEDT precisely matched the reference data. The accomplishments of this research recommend that researchers conduct further study on the highly capricious behavior of weather with the power of the data-science and machine learning technology.

I. Introduction

ACCORDING to the International Air Transport Association (IATA) [1], it is forecasted that the fuel cost will reach $200 billion, accounting for around 24.2% of airline operating expenses in 2019. In conjunction with this trend, Figure 1 [2] also shows the projection of the total number of passengers up to 2038. As air-traffic demand continues to grow, conceivably, various issues may become critical such as airport capacity saturation, operation delay, fuel price, and network impact by airport shutdown due to disastrous weather. These problems should be managed by a variety of aerospace technologies with appropriate regulations. For example, one of the most straightforward solutions could be to optimize the fuel consumption, not only to cope with the dynamically changing market but also to maximize the Revenue Passenger Miles (RPM). As such, it is important to estimate the fuel consumption as accurate as possible since it is critical and has a significant impact on an airline's operation cost.

Since the fuel consumption typically is not publicly accessible, it is usually calculated and analyzed by using a simulation tool. The Aviation Environmental Design Tool (AEDT) is one of the most widely used software that simulates aircraft performance in terms of fuel consumption, emission, and noise. Especially,

[1] Graduate Research Assistant, School of Computational Science and Engineering, AIAA Student Member
[2] Graduate Research Assistant, School of Aerospace Engineering, AIAA Student Member
[3] Research Engineer, School of Aerospace Engineering, Senior AIAA Member
[4] Regent Professor, School of Aerospace Engineering, AIAA Fellow

the AEDT is actively used by the United States (US) government for regulatory studies, research, and domestic aviation system planning, as well as environmental policy analysis [3]. The AEDT is designed to process both terminal and gate-to-gate flights based on highly organized databases for aircraft, airport, runway, and weather. In this paper, we used the AEDT as the main modeling and simulation tool to calculate fuel consumption.

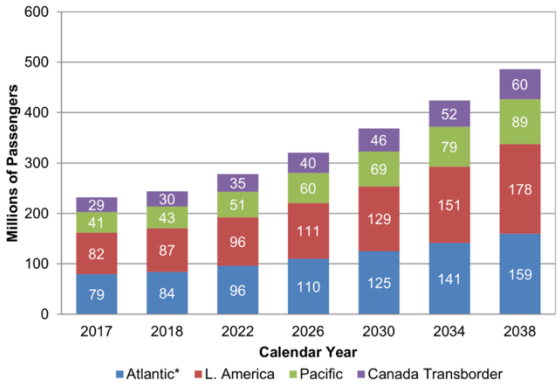

Figure 1. Total passengers to/from US [2]

II. Research Motivation

On February 19th 2019, a flight from Los Angeles (KLAX) to London (KLHR) achieved a record-breaking speed overnight over central Pennsylvania while flying through the jet streak as shown in Figure 2 [4]. As such, winds can be considered as a key parameter in the fuel consumption calculation. In general, the fuel consumption of aircraft includes various factors such as engine specification, takeoff gross weight, flight trajectory, and weather conditions.

In fact, the flight trajectory is varied according to weather condition that may be potentially hazardous to aircraft. For this reason, it is possible that the fuel consumption varies for given aircraft type flying given distance because of the flight trajectory variation. In addition, the weather condition certainly affects the flight trajectory; thus, it is also important to estimate weather condition, especially winds correctly for a fuel consumption estimation. This is because an incorrect wind measurement or assumption can result in an incorrect fuel consumption estimation.

However, it is well known that understanding underlying dynamics and basic physical uncertainty of weather is very challenging. For this reason, weather prediction has drawn lots of attentions in recent years; however, it seems that accurate prediction on weather parameters is still a difficult task due to the dynamic nature of the atmosphere.

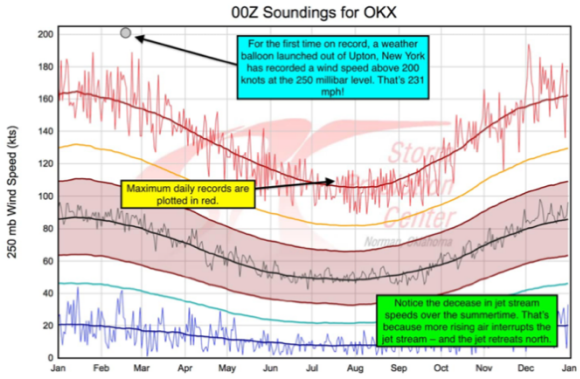

Figure 2. Record-breaking flight with the speed 801 mph [4]

Recently, there has transpired a gigantic paradigm-shift in computer science and engineering due to the debut of machine learning techniques. The impacts have revolutionized both supervised and unsupervised machine learning techniques by outperforming the traditional statistical methods. Moreover, with the significant evolution of data-driven science, machine learning techniques are aggressively harnessed to unravel the hidden dynamics of various complex phenomena. Regarding this paradigm shift, it is hypothesized that the fidelity of established numerical aircraft mission analysis can be improved by uncovering the hidden dynamics of weather using the state-of-the-art machine learning techniques.

In this paper, we proposed a novel aircraft mission analysis framework by incorporating data-driven approaches with the AEDT and one popular supervised machine learning technique, the SVM, to improve the accuracy of aircraft mission analysis.

III. Methodology

A. Data Parsing

1. *FlightAware Live Flight Tracking*

The FlightAware (http://flightaware.com) is a digital aviation company and operates "the world's largest flight tracking and data platform" [sic]. With global connectivity to every segment of aviation, the FlightAware provides over 10,000 aircraft operators and service providers as well as over 12,000,000 passengers with global flight tracking solutions, predictive technology, analytics, and decision-making tools. The FlightAware receives data from air traffic control systems in over 45 countries, the FlightAware's network of ADS-B ground stations in 195 countries, and satellite datalink via every major provider [5]. For free users, the FlightAware provides all tracking information up to the past three months. Its comprehensive dataset contains the time, ground speed, altitude, latitude, longitude, and course with accompanying meta-information such as origin, destination, airline, flight number, and operating aircraft. Moreover, the FlightAware provides an interactive map-based visualization feature to allow users to easily understand how an origin-destination flight operation has been performed. Figure 3 shows the examples of snapshots attained from the live flight tracking feature.

In this paper, we parsed the following real flights from the FlightAware to estimate fuel consumption for the flights. Table 1 shows an example of flight tracking data parsed for one of the flights.

- KATL to KDCA on October 26th 2018
- KSEA to KATL on January 23rd 2019

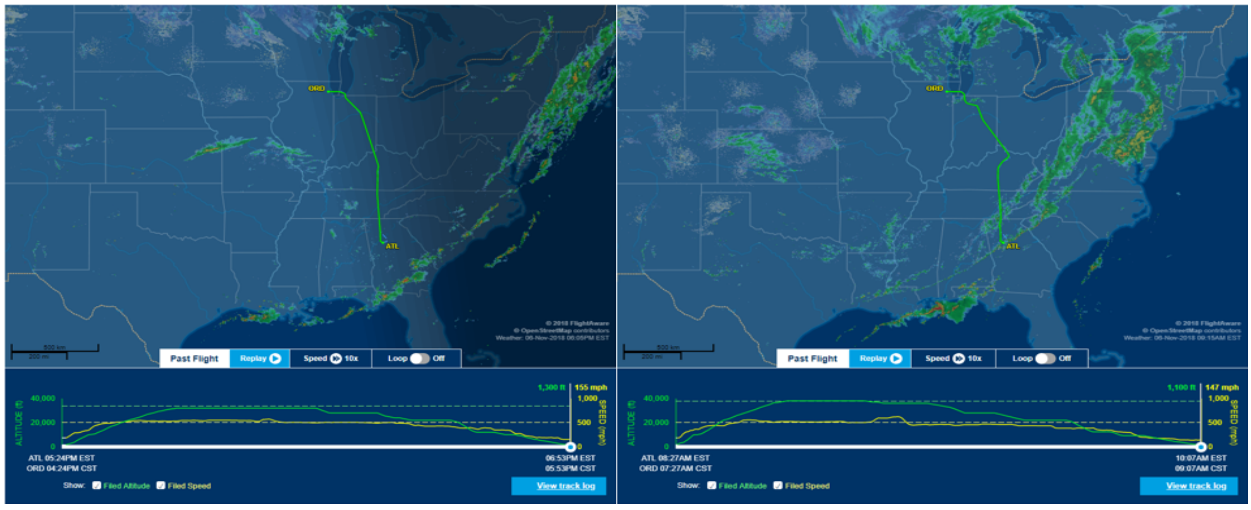

(a) Flight by Delta Airline **(b)** Flight by American Airline

Figure 3. Live track flight tracking service by the FlightAware

Table 1. Small portion of flight track information for DL2775 on January 23rd, 2019

Time (EST)	Latitude (°)	Longitude (°)	Course (°)	Speed (kts)	Altitude (ft)
Thu 01:52:41 AM	47.4243	-122.3083	↓181	170	1,200
Thu 01:52:57 AM	47.4107	-122.3084	↓180	181	1,575
Thu 01:53:13 AM	47.3955	-122.3087	↓181	206	1,700
Thu 01:53:29 AM	47.3811	-122.3092	↓182	225	1,900
Thu 01:53:52 AM	47.3557	-122.3099	↓181	240	2,650
Thu 01:54:10 AM	47.336	-122.3093	↓174	247	3,375
Thu 01:54:42 AM	47.3091	-122.2707	→108	263	4,625
Thu 01:55:01 AM	47.311	-122.2356	→72	274	5,425
Thu 01:55:19 AM	47.3189	-122.204	→71	276	6,175

2. *Modern-Era Retrospective analysis for Research and Applications-2*

The Modern-Era Retrospective analysis for Research and Applications, Version 2 (MERRA-2) is the latest atmospheric reanalysis of the modern satellite era produced by the National Aeronautics and Space Ad-ministration (NASA)'s Global Modeling and Assimilation Office (GMAO) [6]. The MERRA-2 provides a set of detailed weather-related properties, such as temperature, humidity, and wind speed against the 4-D space: longitude, latitude, altitude, and time. Figure 4 shows an example visualization of global eastward wind at a specific time and an altitude by the Panoply tool developed by NASA. In this example, the grid has 576 points in the longitudinal direction and 361 points in the latitudinal direction, corresponding to a resolution of 0.625×0.5 degree.

Since the MERRA-2 has a worldwide weather dataset (the size of the 'daily' MERRA-2 dataset is approximately 1.1GB), we considered only the US contiguous territory as shown in Figure 5. This means that only domestic flights were considered as a case study in this paper. In addition, among various MERRA-2 weather data, we only focused on the eastward and northward wind speed as they are directly related to calculating the true airspeed for the flights of interest.

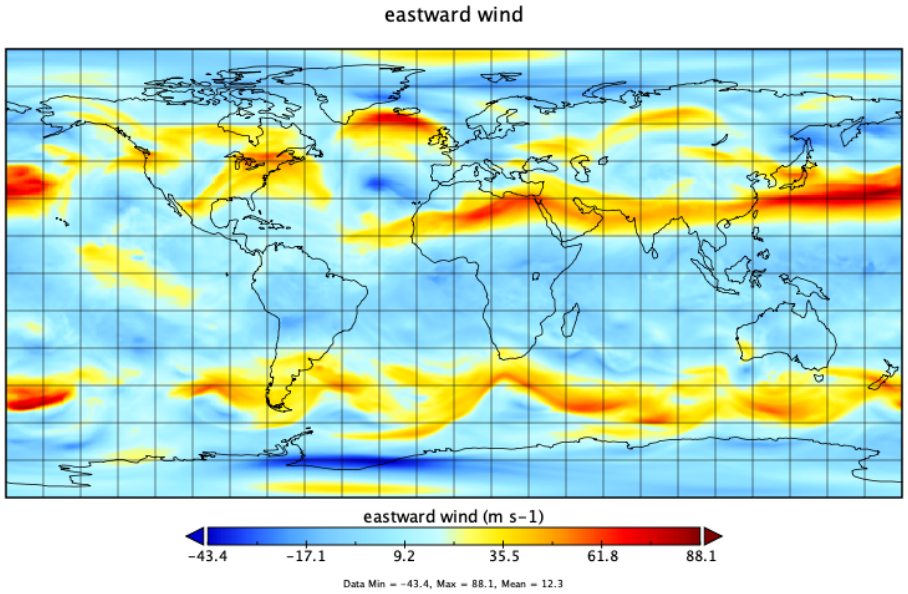

Figure 4. The MERRA-2 weather visualization by the Panoply

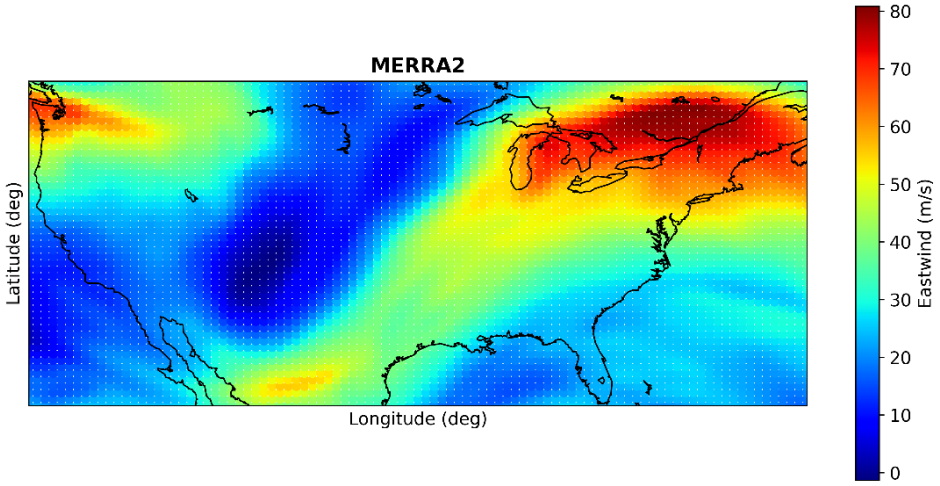

Figure 5. The MERRA-2 weather data pre-processing by the Python

B. Sensor Path Modeling

1. *Sensor Path Generation*

Modeling aircraft performance using the AEDT can be defined as either profile-driven flight performance or trajectory-driven flight performance. For profile-driven flight performance modeling, it describes the movement of aircraft in terms of aircraft state characteristics as a function of horizontal distance over the ground. However, it does not contain information about the lateral path. On the other hand, in terms of trajectory-driven flight performance, it allows for much more freedom in choosing how aircraft will fly because it defines points along the trajectory that the aircraft must pass through [3].

The sensor path modeling, one of trajectory-driven flight performance methods in the AEDT, uses the physical change of state and position of the modeled aircraft to estimate fuel consumption. The input data for operations in the method is intended to come from sensor path sources, such as the Flight Data Record (FDR). In this paper, we parsed 4-D space (e.g. latitude, longitude, altitude, and time) and ground speed information about aircraft from the FlightAware for the sensor path modeling in the AEDT. An overview of sensor path generation process is described in Figure 6. Once the real flight data is retrieved from the FlightAware, data pre-processing is performed to generate an XML file using XML mapping functionality in the Excel. The XML file shown in Figure 7 (a) is then imported into the AEDT with ASIF import option. An example of the sensor path generated in the AEDT for this paper is illustrated in Figure 7 (b).

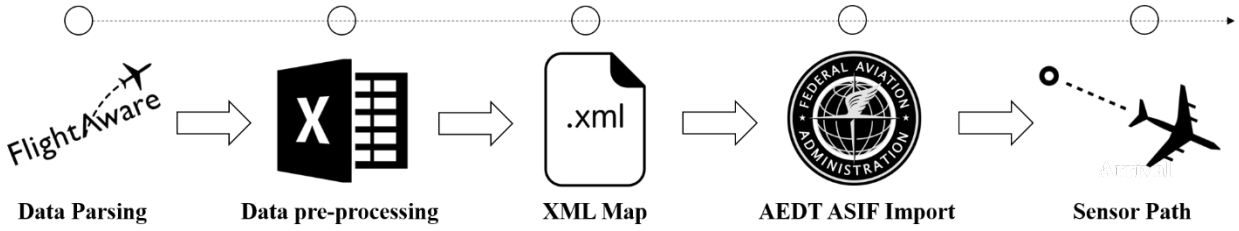

Figure 6. Overview of sensor path generation process

```
<name>DL2775</name>
<source>Aircraft</source>
<startTime>2019-01-23T00:00:00</startTime>
<duration>24</duration>
<description>B737_Flightaware</description>
<trackOpSet>
  <sensorPath>
    <sensorNode>
      <lat>47.4243</lat>
      <long>-122.3083</long>
      <altitude>767.5</altitude>
      <messageTime>2019-01-23T06:52:41</messageTime>
      <sequenceNum>1</sequenceNum>
      <speed>170</speed>
    </sensorNode>
```

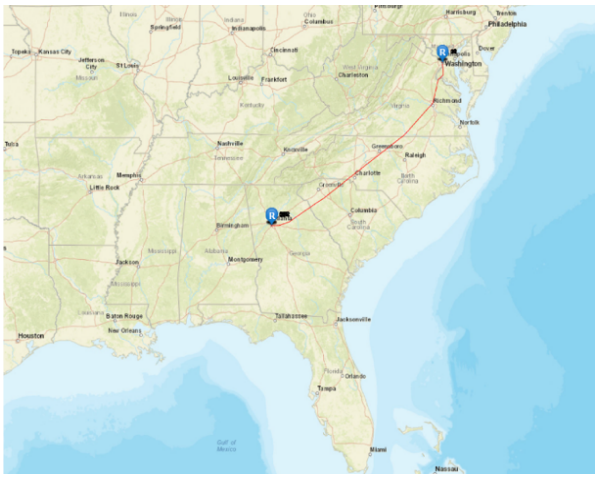

(a) Sensor path XML structure **(b)** Sensor path visualization in the AEDT (KATL to KDCA)

Figure 7. Example of sensor path modeling in the AEDT

2. *Runway Assignment*

To run gate-to-gate flight in the AEDT, it is necessary to assign both takeoff and arrival runway properly. Although the FlightAware provides live flight track information, it does not provide ground roll information about the flight. Hence, the Google Earth software program was used to predict takeoff and landing runway for the particular flights as shown in Figure 8. To be more specific, as can be seen in Figure 8, the FlightAware gives the first point 4-D information after ground roll. Using the information, we could predict both departure and arrival runway and assign the runway information in the AEDT.

Figure 8. Runway prediction by using Google Earth (KATL)

3. *Takeoff Weight Prediction*

The Takeoff Weight (TOW) of an aircraft is an important parameter affecting aircraft performance. It generally impacts a large number of characteristics ranging from the trajectory to the fuel consumption of the flight. However, due to its dependence on factors such as the passenger and cargo load factors as well as operating conditions, the TOW of a particular flight is generally not available to entities outside of the operating airline [7]. For this reason, the AEDT has implemented a representative TOW based on the stage length of the aircraft.

However, it was previously found that the AEDT tends to underestimate the takeoff weights assigned to the different stage lengths [8]. Since the success of fuel consumption calculation relies on the accessibility of reliable TOW data, we used simBrief flight planning database [9], which is based on real-world data, to predict the TOW of a particular flight. Figure 9 shows the estimated TOW for the flight from KATL to KDCA on October 26th, 2018.

```
[ OFP ]
--------------------------------------------------------------------------
DAL2638    26OCT2018     KATL-KDCA    A321 N321SB  RELEASE 0640 19JAN19
OFP 2  HARTSFIELD - JACKSON-RONALD REAGAN WASHINGTON NATL
                         WX PROG 2600 2603 2606    OBS 1900 1900 1900

  ATC C/S    DAL2638       KATL/ATL    KDCA/DCA       CRZ SYS        CI 5
26OCT2018    N321SB        0230/0244   0353/0356      GND DIST        501
A321-200 / CFM56-5B3/P                  STA  0456      AIR DIST        430
                         CTOT:....                     G/C DIST        475
                                                       AVG WIND    269/085
MAXIMUM     TOW 206132   LAW 171520   ZFW 162701       AVG W/C         P062
ESTIMATED   TOW 172800   LAW 165250   ZFW 159141       AVG ISA         P002
                                                       AVG FF LBS/HR 6535
                                                       FUEL BIAS     P00.0
ALTN ....                                              TKOF ALTN     .......
FL STEPS KATL/0330/
```

Figure 9. Takeoff weight prediction using the flight planning database

C. Machine Learning Technique

In general, machine learning can be defined as a category of algorithms that learn from examples and experience in different forms of data, without being explicitly programmed. Among many types of machine learning techniques, we used one supervised learning algorithm called the SVM in this paper.

The basic idea of the SVM is to map the original data into a space by deploying a non-linear kernel trick. In most cases, the SVM is used for a classification problem; however, it can also be used for solving regression problems. In the case of the SVM regression, the goal is to find a function $f(x) = wx + b$ under the condition in which $f(x)$ is within a tolerance ϵ for each data point. To achieve the goal, the SVM performs regression by finding the hyperplane with support vectors that maximize the margin while minimizing the deviation of the data points (i.e. less than ϵ from a real function) depicted as Figure 10.

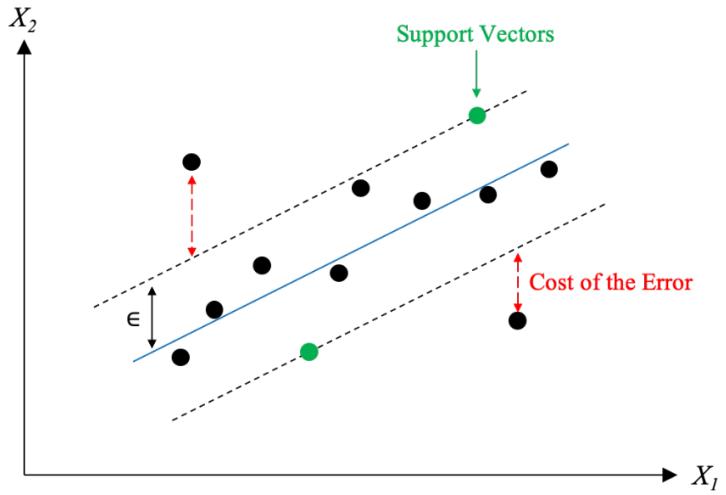

Figure 10. Concept of SVM-based regression

In this paper, the SVM regression technique was used to predict east and north winds using the MERRA-2 weather data due to the following reasons:

- FlightAware provides a real flight trajectory information including ground speed. For sensor path modeling in the AEDT, it is required to specify true airspeed at each flight segment in order to calculate fuel flow rate, which turns out the need for exact wind speed information at the segments.
- The MERRA-2 provides weather data with specific resolutions. For example, the spatial resolution is 0.625×0.5 degrees with respect to longitude and latitude. However, the resolution would not be enough to capture all the points of real flight trajectory, which turns out the need for regression in both time and space.

In response to these concerns, we used the SVM regression technique with the MERRA-2 weather data as shown in Figure 11.

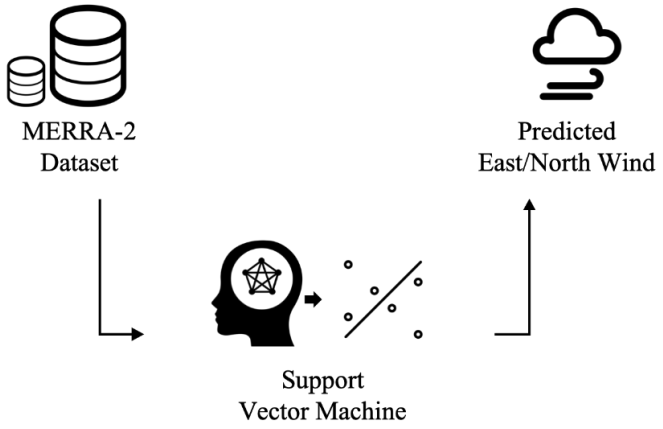

Figure 11. SVM-based regression process used in this paper

In general, a non-linear SVM requires to select a kernel function in order to train the model. After testing a few kernel functions such as polynomial and Radial Basis Functions (RBFs) on the MERRA-2 weather sample data, it was observed that the RBF performs better than other kernel functions; hence, the Gaussian kernel function (or RBF) was utilized to transform the given MERRA-2 to the space.

Figure 12 shows a notional process of the SVM regression with an RBF.

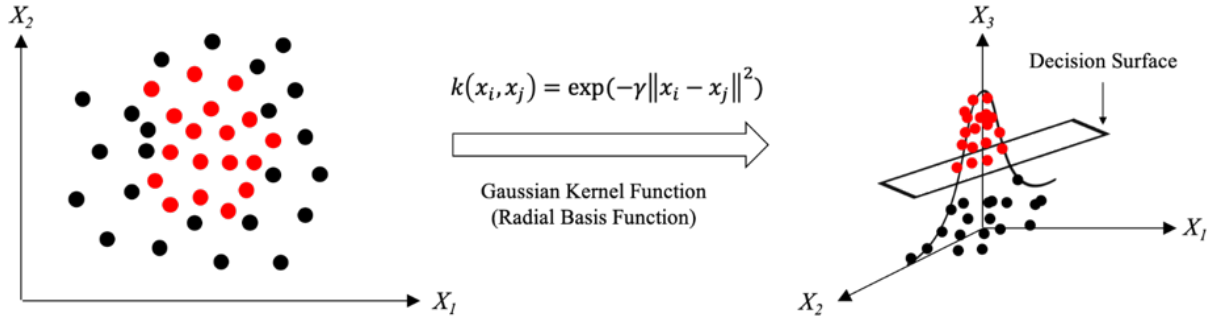

Figure 12. Notional visualization of Gaussian kernel function

IV. Results and Discussions

A. Case Studies

In order to compare the simulation results using the proposed methodology with the reference data, the real flight operations from the FlightAware were compiled with the MERRA-2. The cases are DL2638 from

KATL to KDCA on October 26th 2018 and DL2775 from KSEA to KATL on January 23rd 2019, each of which is shown in Figure 13 and Figure 14, respectively.

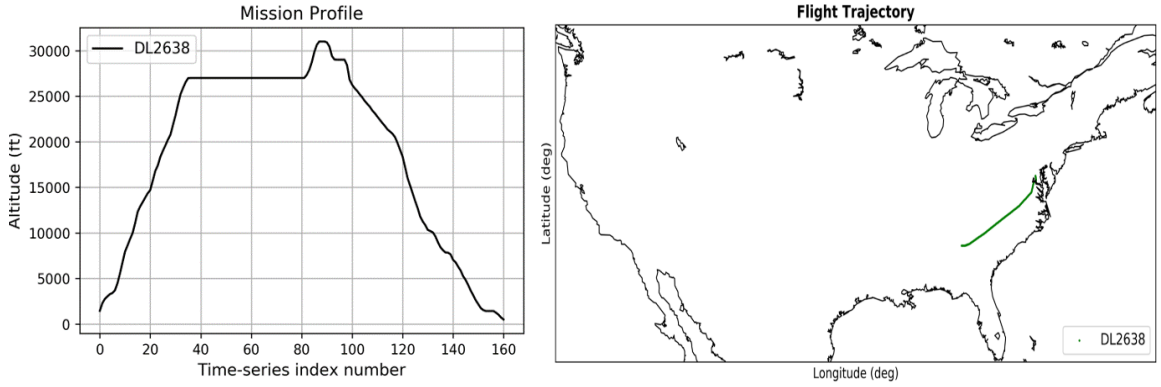

(a) Mission profile **(b)** Flight trajectory

Figure 13. Case study 1: KATL to KDCA on October 26th 2018

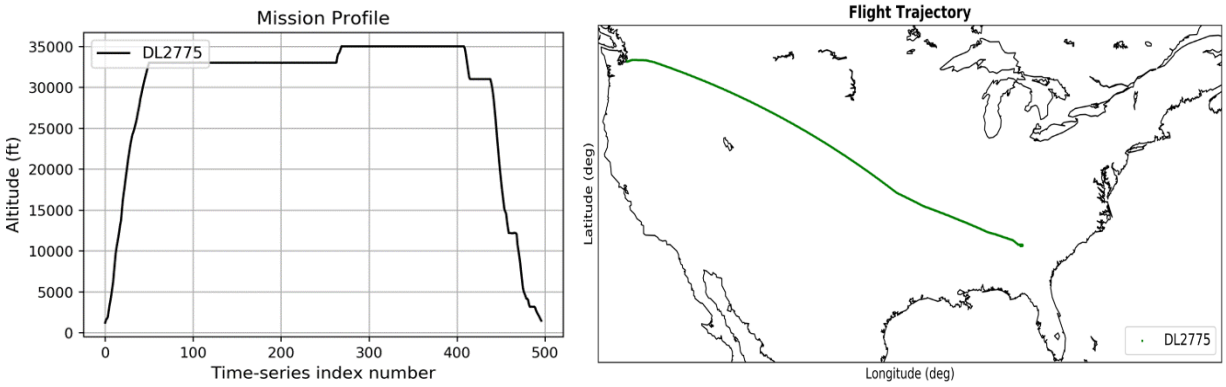

(a) Mission profile **(b)** Flight trajectory

Figure 14. Case study 2: KSEA to KATL on January 23rd 2019

Both Figure 13.(a) and Figure 14.(a) describe mission profile for the particular flight indicating the phases during aircraft mission; whilst Figure 13.(b) and Figure 14.(b) represent the flight trajectory from origin to destination.

B. Weather Prediction by SVM

The MERRA-2 datasets were converted from NetCDF to CSV format using the MATLAB script developed for this paper. After being decomposed into training and validation datasets (80% and 20%, respectively), they were regressed by employed the SVM. Specifically, we modeled two representative dates, October 26th, 2018 and January 23rd, 2019, for both east and north winds. To evaluate the accuracy of the machine learning model, numerical and graphical approaches were employed. In the numerical approach, the coefficient of determination (R^2) and Root Mean Square Error (RMSE) metrics were used. The R^2 represents the variation of response accounted for an approximate model and is given by the equation below:

$$R^2 = 1 - \frac{\sum_{i=1}^{n}(y_i - \hat{y}_i)^2}{\sum_{i=1}^{n}(y_i - \bar{y})^2},$$

where y_i and $\hat{y}_i$ denote exact and predicted response, respectively, and $\bar{y}$ is the mean value of exact responses. The RMSE shows how spread out the residuals are and is calculated by:

$$\text{RMSE} = \sqrt{\frac{\sum_{i=1}^{n}(y_i - \hat{y}_i)^2}{n}},$$

where n is the number of samples. The results are tabulated in Table 2. As can be seen, the higher value of R^2 and lower value of RMSE indicate the developed SVM models are quite accurate.

Table 2. Numerical validation of SVM models for January 23rd, 2019

	East wind		North wind	
	R^2	RMSE	R^2	RMSE
Training	0.9939	0.7875	0.9910	1.0445
Validation	0.9927	0.9837	0.9965	2.0136

In the graphical approach, the Actual by Predicted plot was generated to determine how well the response is approximated by the model. As shown in Figure 15, actual responses are mostly on top of predicted ones and they are randomly scattered along the perfect fit line. Moreover, the residual histogram plots were created to display the distribution of the residual. As a result, it was notable that a certain amount of skewness is observed. For instance, it was found that the negative error is concentrated on high-speed region as shown in Figure 15 (b). Concerning this, it is possibly claimed that the relative error between the actual speed and predicted one was small under the existence of skewness, typically between -5 and 0.

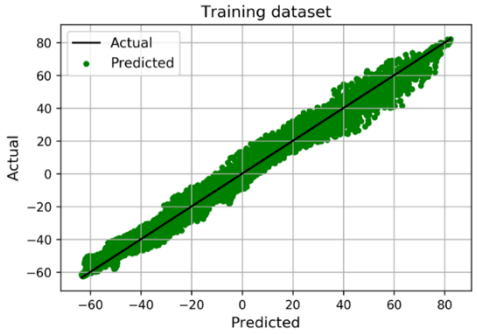

(a) Actual versus predicted plot: training data

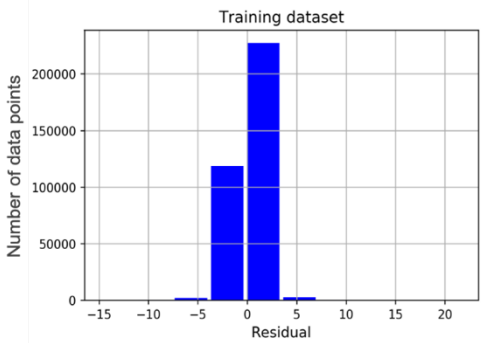

(b) Residual histogram plot: training data

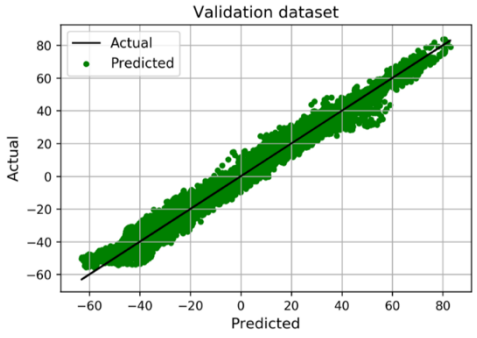

(c) Actual versus predicted plot: validation data

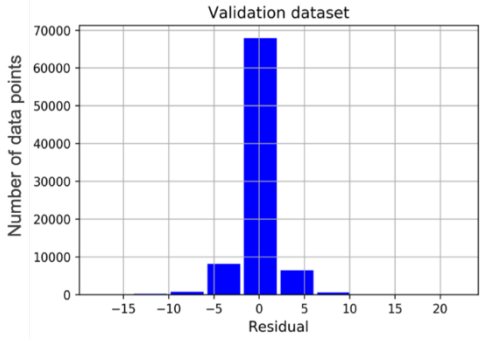

(d) Residual histogram plot: validation data

Figure 15. Graphical validation of the SVM north wind for January 23rd, 2019

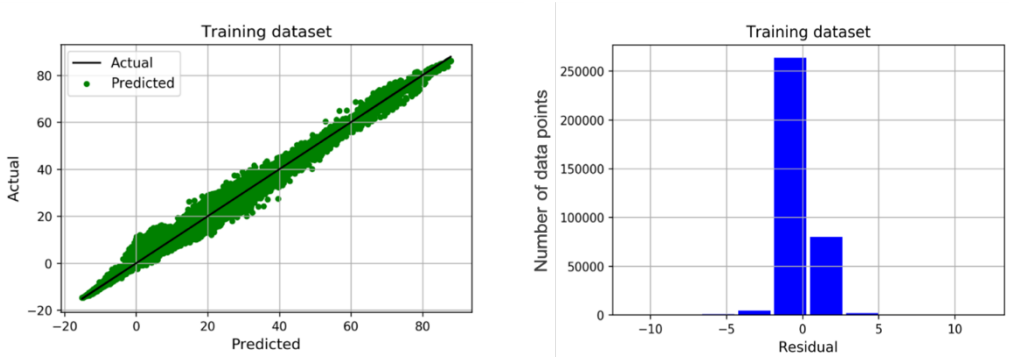

(a) Actual versus predicted plot: training data **(b)** Residual histogram plot: training data

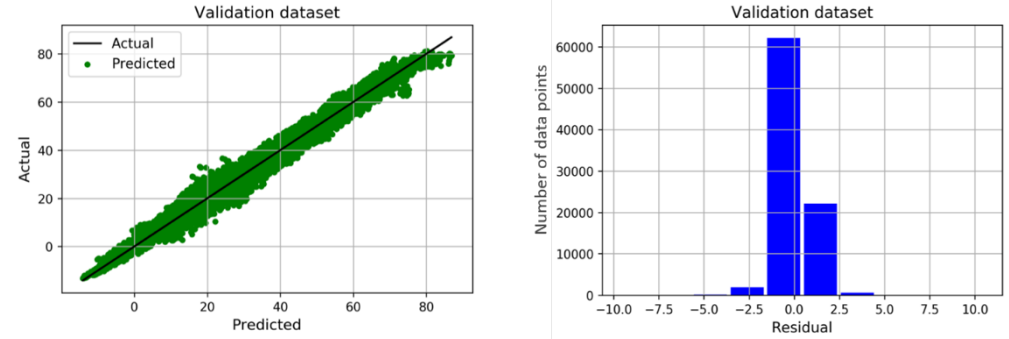

(c) Actual versus predicted plot: validation data **(d)** Residual histogram plot: validation data

Figure 16. Graphical validation of the SVM east wind for January 23rd, 2019

Additionally, the MERRA-2 datasets were compared against the datasets generated by the SVM models with respect to east and north wind values. Figure 17 and Figure 18 depict contours for east and north winds at 4:00 AM (EST) on January 23rd 2019 at which the altitude is 33,894 ft.

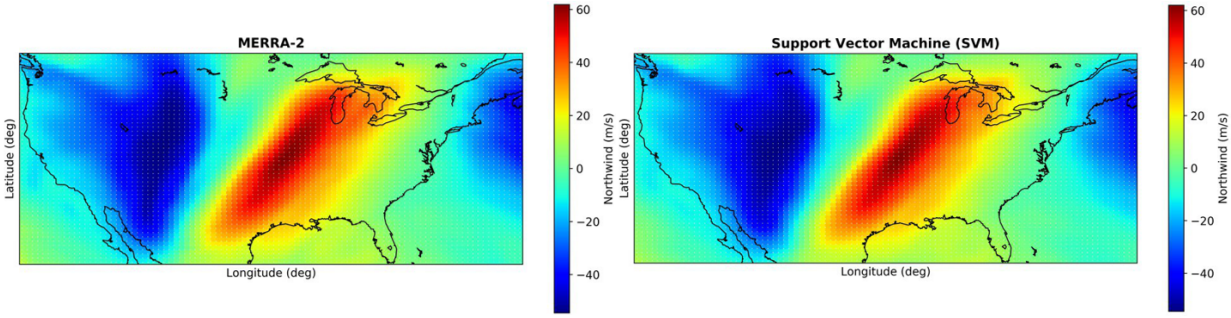

(a) MERRA-2 north wind **(b)** SVM north wind

Figure 17. Contour comparisons for January 23rd, 2019 (North wind)

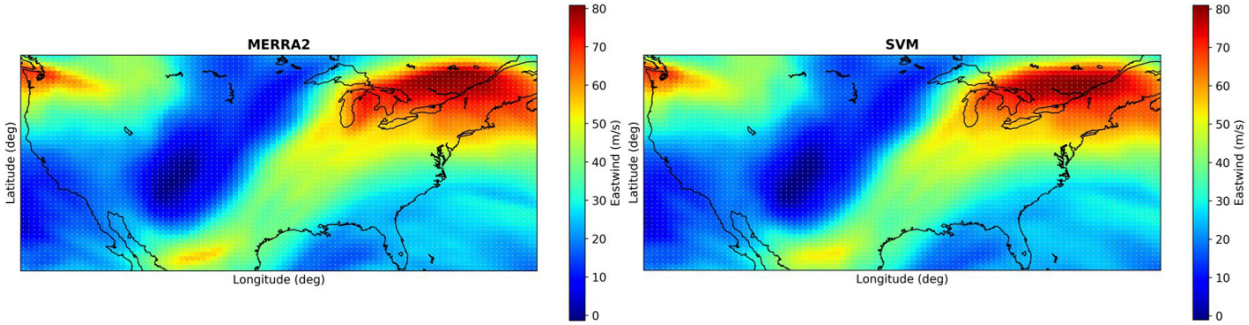

(a) MERRA-2 east wind **(b)** SVM east wind

Figure 18. Contour comparisons on January 23rd, 2019 (East wind)

As the final procedure of validation, another weather reference data from the aircraft report in National Oceanic and Atmospheric Administration (NOAA) Aviation Weather Center [10] was employed. Figure 19 notionally illustrates how the sample points are decomposed to training, validating, and testing.

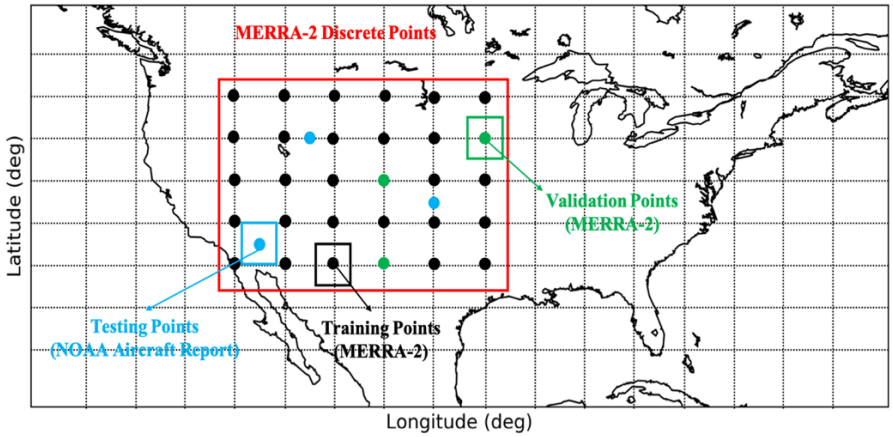

Figure 19. Dataset description for SVM machine learning model

Table 3 and Table 4 compare the SVM model against the aircraft-reported weather. An intriguing observation can be made; the predicted weather values above 30,000 ft are more accurate than those of below 30,000 ft. In subsequent sections, these two sub-airspaces will be referred to as H-space (higher airspace) and L-space (lower airspace), respectively.

Table 3. SVM east wind validation against testing data for KSEA-KATL

Time (GMT)	Latitude (°)	Longitude (°)	Altitude (ft)	Actual east wind (m/s)	SVM east wind (m/s)	Absolute Difference (%)
22:40:00	36.7484	-108.0990	10,000	10.2463	9.4901	7.97
15:20:00	43.1	-78.7	24,000	37.7067	34.6691	8.76
23:32:00	32.7167	-97.9833	29,000	21.0528	19.7646	6.52
14:59:00	40.9667	-78.8333	30,000	51.3762	52.8362	2.84
21:45:00	31.0167	-98.0833	31,000	20.2066	19.8765	1.63
19:54:00	42.6833	-69.0667	33,600	54.9135	55.2869	0.67
12:32:00	39.6925	-73.5373	34,000	48.3944	47.9042	1.01
20:20:00	37.0333	-100.967	34,000	16.9439	16.4696	2.79

Table 4. SVM north wind validation against testing data for KSEA-KATL

Time (GMT)	Latitude (°)	Longitude (°)	Altitude (ft)	Actual north wind (m/s)	SVM north wind (m/s)	Absolute Difference (%)
18:11:00	30.8762	-82.2263	10,000	15.1672	16.4653	7.88
16:20:00	31.8670	-84.2286	14,000	19.7043	21.0499	6.39
15:53:00	43.1	-78.7	24,000	13.7241	14.6354	6.23
12:12:00	41.2253	-71.4412	28,000	-4.5987	-4.4836	2.50
17:49:00	37.6667	-90.2333	30,000	56.9382	57.5926	1.15
07:16:00	33.4833	-122.5830	32,000	-11.8393	-11.5780	2.20
01:53:00	37.4833	-71.4500	34,000	-23.8330	-23.1499	2.86
21:25:00	38.9333	-104.6330	35,000	-23.0211	-22.9104	0.48

In order to take a deep dive into the dynamics of the discernible difference of accuracy, the relative error of each wind at a single point, $E_w(t, a, ln, lt)$, was calculated by the equation below:

$$E_w(t, a, ln, lt) = \min\left(\left|\frac{V_{a,w}(t,a,ln,lt) - V_{p,w}(t,a,ln,lt)}{V_{a,w}(t,a,ln,lt)}\right|, 0.2\right) \times 5,$$

where $w \in \{e\ (\text{east wind}), n\ (\text{north wind})\}$, t, a, ln, lt represent wind direction, altitude, latitude, longitude, and time, respectively. Also, $V_{a,w}$ and $V_{p,w}$ mean the actual and predicted velocities, respectively. Note that the error was normalized in a range [0, 1] and all relative errors which are larger than 20% were set as the maximum, which is 1, by applying a simple mathematical limiter to remove all distinguishable outliers. The 20% maximum value was determined considering the distribution of the data. Finally, the relative error at longitude *i* and latitude *j* averaged about *t* and *a*, $E_{avg}(i, j)$, is represented as four different shapes by the following equation:

$$E_{avg}(i,j) = \begin{cases} \dfrac{\sum_{t=1}^{8}\sum_{a=13}^{20} E_e(t,a,i,j)}{8 \times 8} & \text{east wind of L-space} \\ \dfrac{\sum_{t=1}^{8}\sum_{a=20}^{23} E_e(t,a,\ i,j)}{8 \times 4} & \text{east wind of H-space} \\ \dfrac{\sum_{t=1}^{8}\sum_{a=13}^{20} E_n(t,a,\ i,j)}{8 \times 8} & \text{north wind of L-space} \\ \dfrac{\sum_{t=1}^{8}\sum_{a=20}^{23} E_n(t,a,i,j)}{8 \times 4} & \text{north wind of H-space} \end{cases},$$

where $t \in \{1, 2, 3, \cdots, 8\}$ and $a \in \{13, 14, 15, \cdots, 23\}$ represent the indices of time (three-hour interval) and altitude in the MERRA-2, respectively. The minimum ($a = 13$) and maximum ($a = 23$) of altitude are 9,878 ft and 38,615 ft, respectively, while the airspace is evenly discretized. Figure 20 notionally delineates the overall division of airspace in conjunction with corresponding average error information tabulated in Table 5.

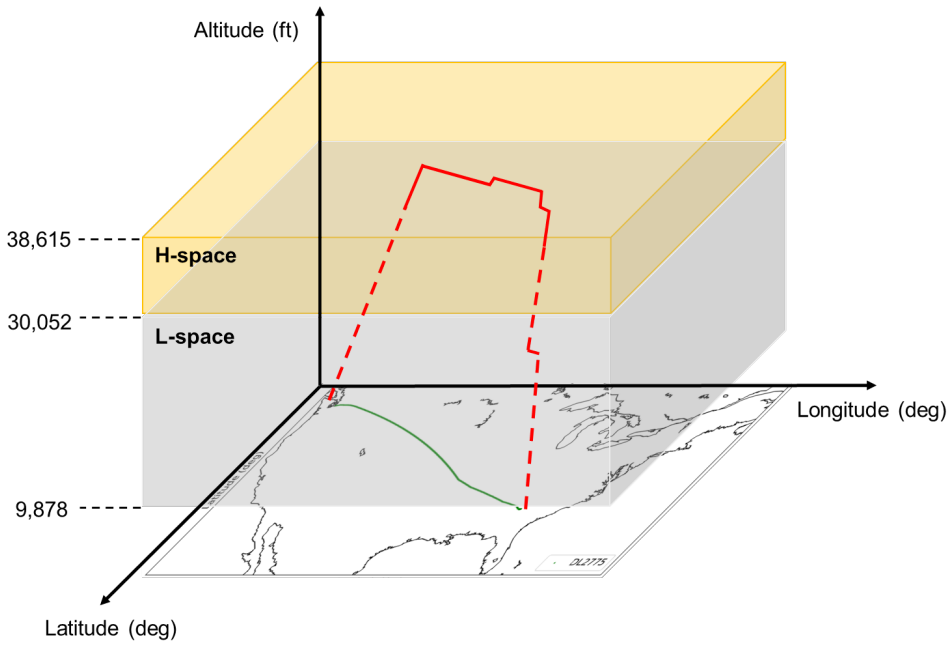

Figure 20. Notional delineation of airspace decomposition (L-space & H-space)

Table 5. Average relative error (E_{avg})

Cases	East Wind (%)	North wind (%)
L-space	8.48	12.46
H-space	2.84	7.32

As conceived in Table 5, the SVM model better predicted typically in H-space. To identify the exact mechanism should require an additional in-depth investigation. However, it is clearly beyond the research scope of this paper such that a detail exploration of this phenomenon will be conducted in future research pathway.

In order to better represent the relative error, Figure 21 was created to compare the L-space and H-space. As implemented in the corresponding equation, the value reaches between [0, 1] for fair comparison under the same condition. Note that the white solid line is the trajectory of the flight from KSEA to KATL on January 23rd, 2019.

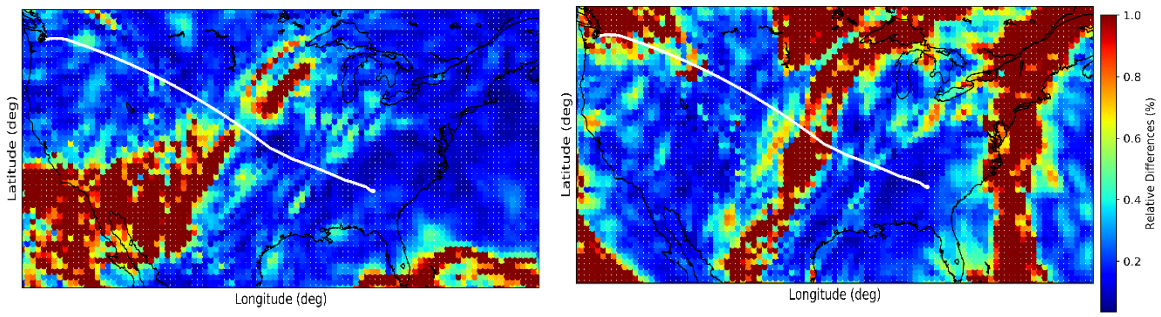

(a) East wind in L-space **(b)** North wind in L-space

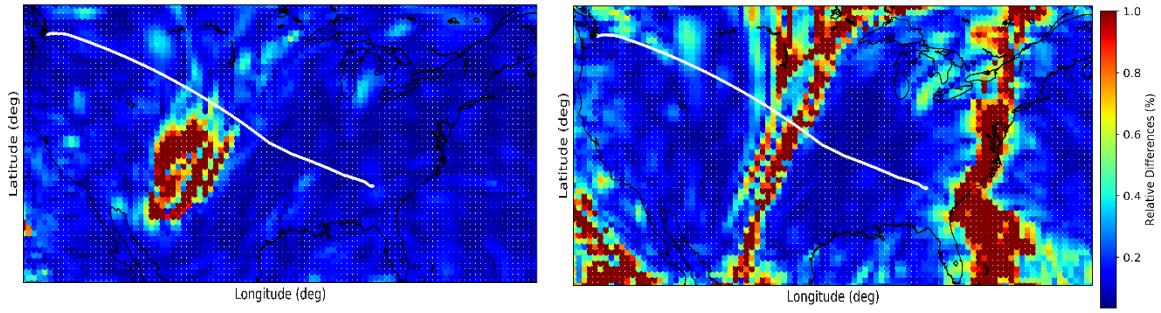

(c) East wind in H-space **(d)** North wind in H-space

Figure 21. Contour plots of average relative error

One can identify the unequivocal difference of the average relative errors of both airspaces via these contours more clearly than through Table 5. Likewise, this discussion inspires us in figuring out two major insights. First, the SVM surrogate model always has better predictive power in east wind than in north wind. The average relative error of east wind is smaller than that of north wind in all airspaces. In a physical perspective, east wind is the dominant one so that it is hypothesized that the more-accurate east wind would have contributed to the enhancement of fidelity in aircraft mission analysis. Second, focusing on the east wind, the SVM model shows better accuracy typically in H-space, which over 30,000 ft. Considering the mission profile, the cruise flight takes most of the mission profile and is performed in approximately around 35,000 ft. Thus, it is highly claimed that the 'relatively' more accurate weather prediction in H-space would also be another potential contributor that could enhance the fidelity in estimating aircraft fuel burn.

Finally, it is also discussed that the flight trajectory in the figure does not fly over the region where the average relative error is close to 1, which is the largest. This observation addresses an intriguing conjecture; the larger amount of the average relative error might be more correlated to the non-linear characteristics of weather rather than the smaller value since the more non-linear the weather is, the more difficult the SVM can capture the behavior. However, it is modestly surmised that the flight trajectory might be qualitatively optimized; at least it seems that the aircraft circumvents the region where the non-linear behavior of the weather is strong. Certainly, this must be confirmed through a further research effort.

C. Fuel Consumption Estimation

Once the physical changes of state and position of user-defined aircraft are fed into the AEDT, the AEDT calculates the fuel flow over each consecutive trajectory point. In this paper, we explored two popular civil trajectories for test cases: 1) KATL to KDCA and 2) KSEA to KATL. Figure 22 illustrates the entire overview of the proposed methodology we developed for this paper.

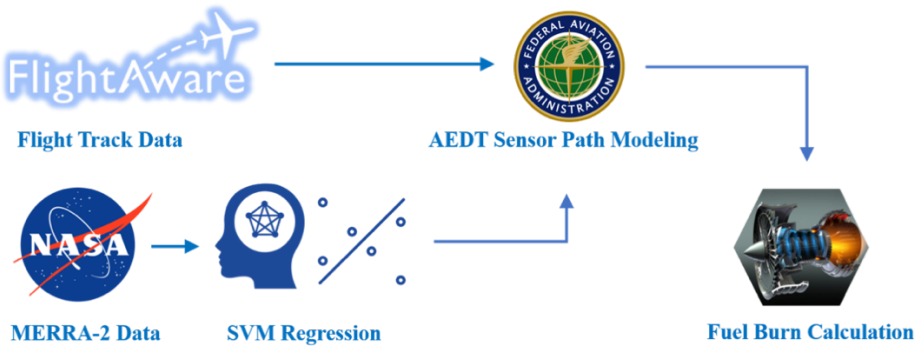

Figure 22. Overview of the proposed methodology

The tabulated fuel burn estimations in Table 6 and Table 7 show a good agreement with the reference data (Note that the values were normalized due to a proprietary concern); however, small differences still

exist between simulation and the reference values. The sources of these discrepancies can result from the following possible assumptions or simplifications:

- The taxi fuel consumption was not included.
- There were model regression errors.
- Only the weather above 10,000 ft was regressed to reduce computational costs for training MERRA-2 weather datasets.
- The takeoff weight might be still inaccurate even if it was predicted from real world-based flight planning tool.

Furthermore, it is conjectured that the case study 2 would possibly yield a better result in its fuel consumption calculation because the accuracy of the SVM model is typically better in high altitudes than low altitudes. In other words, it would be expected that the fidelity of the AEDT is enhanced for a flight whose cruise segment is dominated.

Table 6. Case study 1: KATL to KDCA on October 26th 2018

Case	Fuel Burn (lbs)	Absolute Difference (%)
Proposed methodology	1.09	9.4
Reference	1	N/A

Table 7. Case study 2: KSEA to KATL on January 23rd 2019

Case	Fuel Burn (lbs)	Absolute Difference (%)
Proposed methodology	1.05	5.5
Reference	1	N/A

V. Conclusion

In this study, we proposed a novel aircraft mission analysis framework by incorporating data-driven approach with the AEDT. To enhance the fidelity of aircraft mission analysis in the existence of weather uncertainty during airborne, an ML technique was utilized. As the organized weather information, the MERRA-2 and aircraft reports were gathered from the NASA and the NOAA, respectively; the former was used to train and validate the SVM model enveloping the mainland of the US with selected ranges of altitudes and the latter was used for testing the SVM model. For the concept of implementation, several public flight trajectories (KATL-KDCA, KSEA-KATL) were acquired from the FlightAware. The accurately regressed weather data successfully collaborated with the AEDT, resulting in an enhanced fidelity for the test cases.

In conclusion, the accomplishment of this paper can be implemented in estimating the fuel consumption of other flight paths in future research involving more flight data as well as elaborated regression approaches. For example, another public weather data High-Resolution Rapid Refresh (HRRR) from the NOAA provides an hourly-basis dataset of weather, whereas the MERRA-2 has a three-hour interval. Thus, if the HRRR is considered to be employed in future research, a more in-depth data space exploration and analysis tasks may be required considering the trade-off between computational cost and accuracy in various supervised machine learning techniques to deal with the much larger amount of dataset than that of the MERRA-2.

VI. References

[1] IATA, "Fuel Fact Sheet", *IATA Airline Industry Economic Performance,* December 2018.

[2] FAA, "FAA Aerospace Forecast Fiscal Years 2018-2038", *U.S. Department of Transportation,* 2018.

[3] FAA, "AEDT 2d Technical Manual", *U.S. Department of Transportation, September* 2017.

[4] Matthew Cappucci, "Flight reaches 801 mph as a furious jet stream packs record-breaking speeds", URL: https://www.washingtonpost.com/weather/2019/02/19/flight-reaches-mph-furious-jet-stream-packs-record-breaking-speeds/?fbclid=IwAR1UuO_gTGBrrEoA-3v7CUSBBMVrdOnaNvnyvzOMh0tPKqsvGVpxTlFWQys utm_term=.3455e34b15bd [cited April 2019].

[5] FlightAware, "About FlightAware", URL: http://flightaware.com [cited April 2019].

[6] Ronald Gelaro, "The Modern-Era Retrospective Analysis for Research and Applications, version 2 (MERRA-2)", *Journal of Climate,* 30(14): 5419-5454, 2017.

[7] Yashovardhan S Chati and Hamsa Balakrishnan. Modeling of aircraft takeoff weight using gaussian processes. *Journal of Air Transportation*, 26(2):70–79, 2018.

[8] Dongwook Lim, Matthew J LeVine, Vu Ngo, Michelle Kirby, and Dimitri N Mavris. Improved aircraft departure modeling for environmental impact assessment. In *2018 Aviation Technology, Integration, and Operations Conference*, page 3503, 2018.

[9] Derek Mayer, "About simBrief", URL: http://www.simbrief.com [cited April 2019].

[10] National Oceanic and Atmospheric Administration, "HRRR weather", URL: https://rapidrefresh.noaa.gov/hrrr [cited April 2019].